Studying Chromium and Nickel Equivalency to Identify Viable Additive Manufacturing Stainless Steel Chemistries

Zachary T. Hilton, Joseph W. Newkirk, Ronald J. O'Malley

Department of Materials Science and Engineering, Missouri University of Science and Technology, Rolla, MO 65409

Chromium and nickel equivalency modeling has long been used in welding to determine the weldability of steel chemistries. A study was conducted to determine the applicability of Cr-Ni modeling to the additive manufacturing process. Many AM methods involve rapid solidification of small melt pools, similar to welding. Chemistries with varying Cr/Ni ratios were selected for use in a selective laser melting process and modeled using known models. Initial results indicate that the standard "safe welding zone" may not directly apply to additive manufacturing. The capability to build with chemistries outside the weldability "safe zone" could result in improved and varied properties for additively manufactured materials.

Introduction

Many of the alloys currently in use in the additive manufacturing (AM) industry were developed for use in other industries, such as casting. As such, only minor work has been done to create alloys tailored specifically to addressing the needs and issues unique to the additive manufacturing industry. With the final goal of tailoring a 304L-like stainless steel alloy composition specifically to AM processes, an initial study was conducted. This initial study was conducted to determine if weldability, determined via Cr/Ni modeling, was a useful metric for determining a chemistry's build viability.

To determine whether weldability can be used to determine build viability, a 304L powder composition was acquired and the Cr/Ni equivalency values were calculated for that chemistry. Cr/Ni equivalency values were then plotted on a modified Schaeffler diagram, modified as detailed in WRC-1992 paper, in order to predict the alloy's solidification mode [1, 2]. JMatPro simulations were also run to verify the predicted solidification mode and to determine additional phases that could potentially form. The Cr/Ni equivalencies of the alloy were then modified by blending it with varying amounts of 316L powder. JMatPro simulations and a modified Schaeffler diagram, modified as detailed in the paper by Suutala, were then used to select which ratios would be tested in builds. The selected ratio powder blends were then built into parts using identical build parameters and a series of tests were performed on the build in order to determine whether weldability can be used to determine build viability. The following is a discussion of the preliminary results of this study and for this preliminary study, build viability is defined by the appearance of detrimental phases and excessive cracking. After testing these preliminary results suggest that weldability may not be the sole parameter that needs to be considered when determining build viability. The authors are not currently aware of similar studies related to stainless steel alloy optimization for AM processes.

Methodology

A 304L stainless steel powder was acquired from LPW Technology with the composition reported in Table 1. Once the composition of the powder was known, the Cr/Ni equivalency values were calculated. There are a number of different methods for calculating the Cr/Ni equivalency values; however, for this study the equations referred to as the WRC-1992 equations, shown in Table 1, were used [1, 2, 3]. The Cr/Ni equivalency values were also calculated using the Hull and Delong equations, but for consistency, only the WRC-1992 calculated values will be discussed [4, 5]. The WRC-1992 equations are used as they allow for accurate predictions of the ferrite number of a larger range of alloys without varying significantly from the predictions of the more specific models [3].

Table 1: Composition of 304L Powder Used and WRC-1992 Cr/Ni Equivalency Equations and Values.

C (Wt%)	Mn (Wt%)	S (Wt%)	Si (Wt%)	Cu (Wt%)	Ni (Wt%)	P (Wt%)	Cb (Wt%)	Cr (Wt%)	O (Wt%)	N (Wt%)
.015	1.40	.0040	.63	.05	9.90	.012	.000	18.50	.0200	.090

Cr_{Eq} =	Cr + Mo + 0.7Cb	= 18.50
Ni_{Eq} =	Ni + 35C + 20N + .25 Cu	= 12.24

After calculating the Cr/Ni equivalency values for the composition, the values were plotted on a WRC-1992 modified Schaeffler diagram, shown in Figure 1. The diagram was used as a tool for predicting the amount of delta ferrite present in the powder and the powder's solidification mode [2, 3]. To help confirm the solidification mode predictions, carbon isopleth and TTT diagram simulations were run using JMatPro v9.1. Figure 2 shows the predicted carbon isopleth diagram and Figure 3 shows the predicted TTT diagram for the powder composition in Table 1. Through the use of the Suutala modified Schaeffler diagram, shown in Figure 4, it was also determined that this particular composition of powder resided within a "safe welding zone" [2]. This "safe welding zone" was developed using thermodynamic modeling and empirically determined equations for Cr/Ni equivalency with observations from welding tests [2, 6].

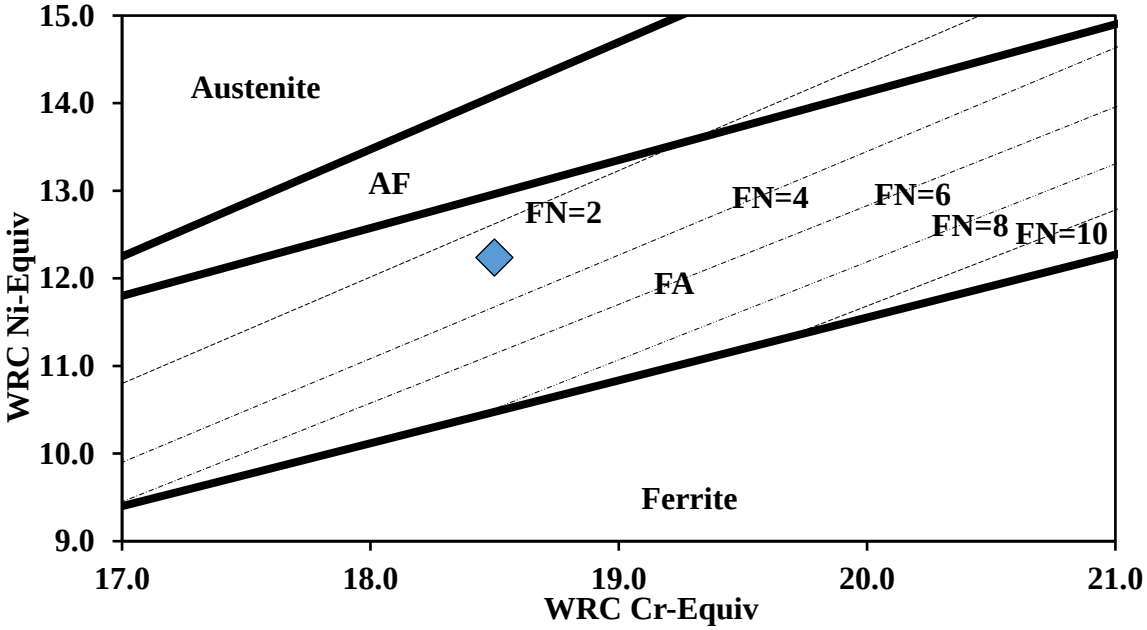

Figure 1: A Schaeffler diagram displaying the location of the 304L powder composition used [3].

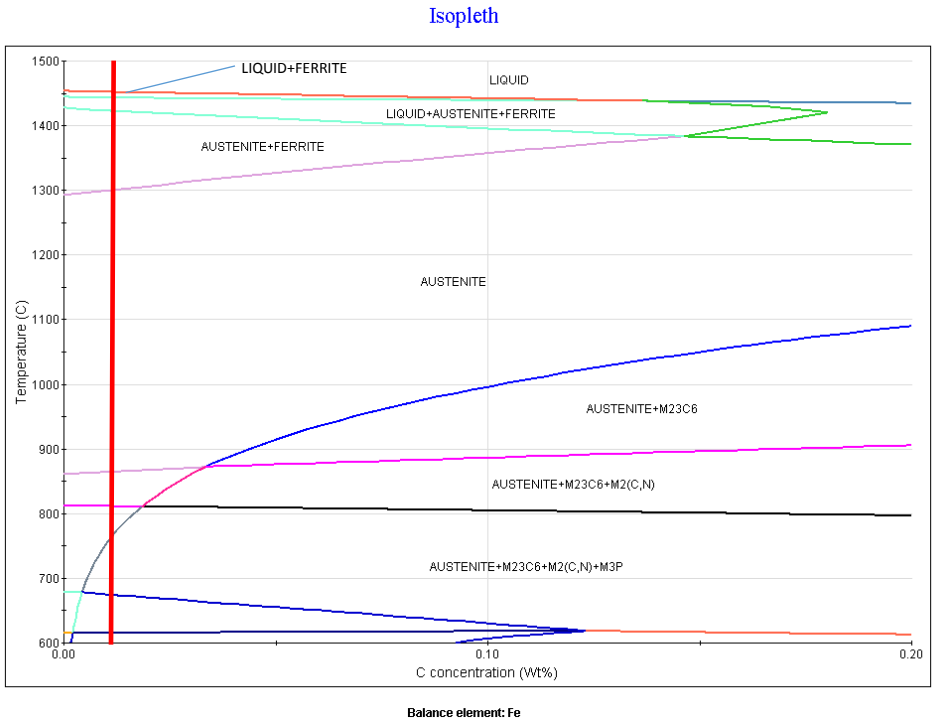

Figure 2: The predicted carbon isopleth diagram for the 304L powder composition used. The red vertical line indicates the approximate amount of carbon in the composition. The unlabeled lower phases contain ferrite as well as austenite and the labeled carbides, and phosphides.

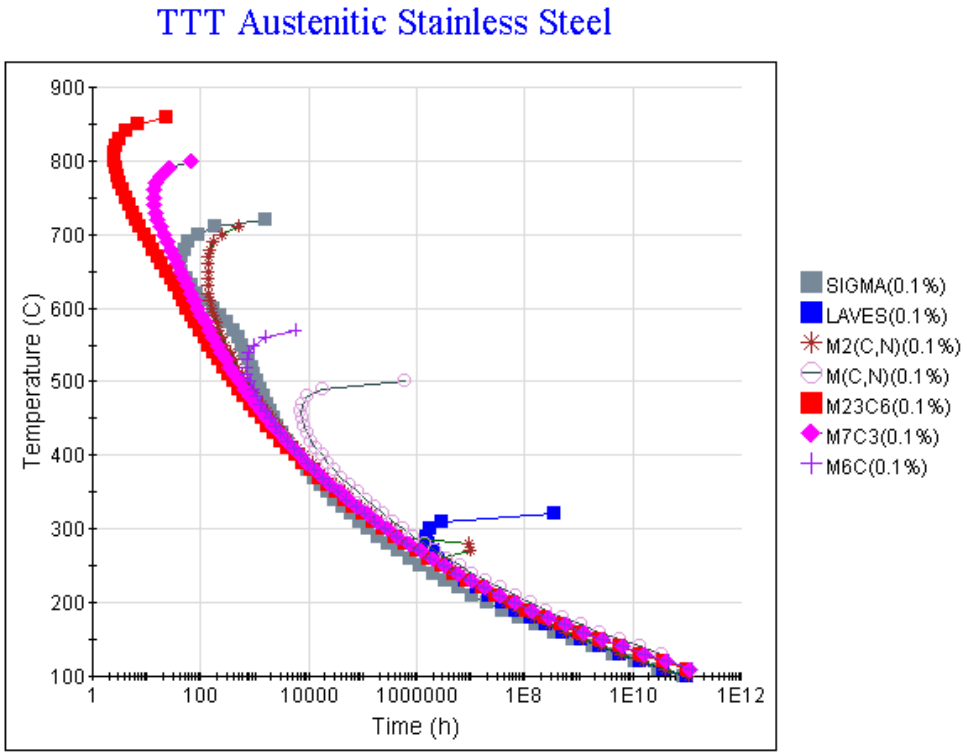

Figure 3: The time-temperature-transformation diagram for the 304L powder used. It is important to note that the sigma, chi, and Laves phases are predicted to be very slow forming.

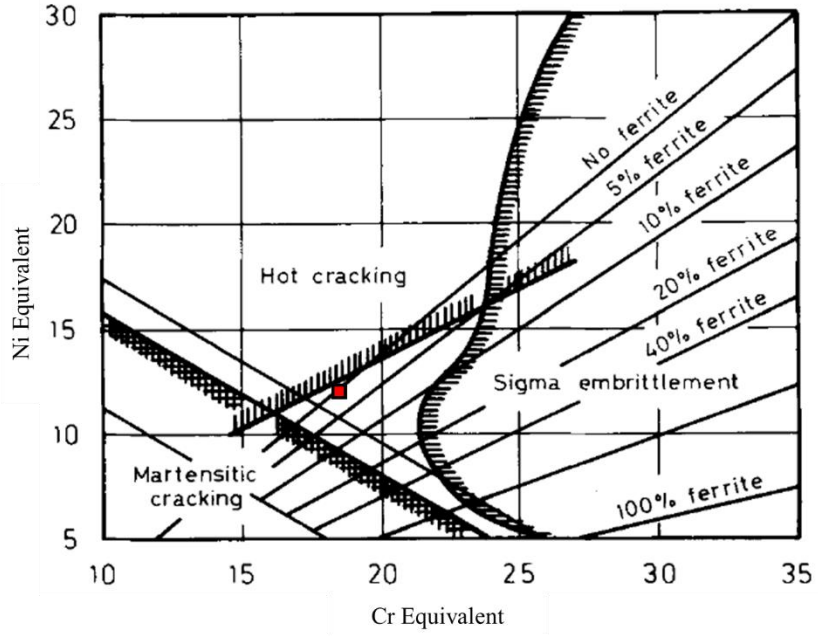

Figure 4: A Schaeffler diagram modified specifically for the purpose of assisting in the determination of a material's weldability [2].

In order to test the effect of Cr and Ni equivalency on the build viability of different powders, the concept of using blended powders was used in order to acquire preliminary results and determine an effective testing strategy. A previously acquired 316L powder composition was selected as the second blend powder for the 304L powder. The exact composition of the 316L powder is currently unknown, so a nominal composition was acquired from Aerospace Specification Metals Inc [7]. These chemistries were used as a predictive tool, the exact chemistries used were then determined using an arc spectrometer and optical emission spectroscopy (OES). The carbon and nitrogen values were confirmed using Leco CS 600 and TC 500 combustion analyzers, respectively. In to maximize the range of chemistries tested and minimize powder usage, it was decided that only three specific blends would be tested. The three blends were selected by examining their position on the Suutala modified diagram and their susceptibility for detrimental phase formation. The positions of the three blends on the Suutala modified diagram are shown in Figure 5 and the compositions, determined via OES and combustion analysis, are presented in Table 2 along with the nominal 316L composition used in the predictive calculations. TTT diagrams were generated using JMatPro for the three selected powder blends. The TTT diagrams were used as a means of approximating a composition's susceptibility to forming detrimental phases as the Cr/Ni equivalency increased, the time to form detrimental phases decreased.

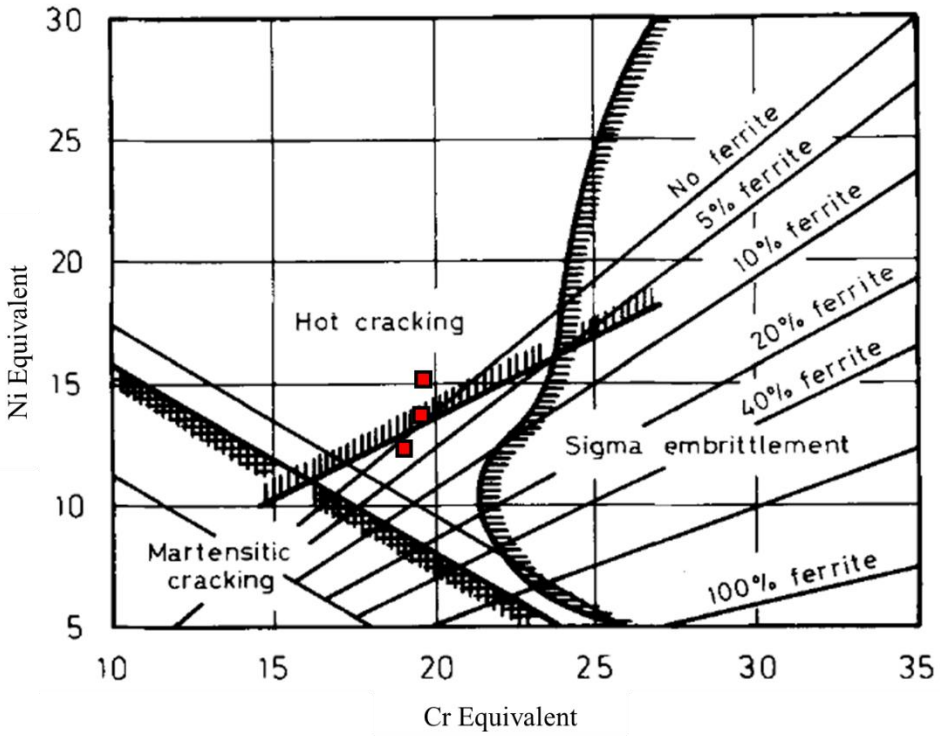

Figure 5: A modified Schaeffler diagram displaying the approximate locations of the three blended powder compositions.

Table 2: Compositions of the Three Powder Blends Used and the 316L Composition Used in the Predictive Calculations with Cr/Ni Equivalency Values.											
	Chemical Composition (Wt%)										
Blend	C*	Mn	Si	Cu	Ni	Mo	Nb	Cr	N*	Cr_{Eq}	Ni_{Eq}
10% 316L	0.0155	1.400	0.641	0.024	10.40	0.217	0.0020	18.50	0.0225	18.72	12.91
60% 316L	0.018	0.877	0.631	0.031	11.20	1.500	0.0020	17.70	0.0100	19.20	13.84
90% 316L	0.0195	0.751	0.749	0.078	12.65	2.290	0.0088	17.00	0.0025	19.30	15.50
100% 316L	0.020	1.330	0.650	0.030	12.70	2.330	0.0020	17.80	0.0000	20.13	15.21

* These values were determined via combustion analysis.

Once the blend compositions were selected the powders were blended by mixing the powders according to the appropriate weight ratios. After the mixing process, the powders were homogenized using a Turbula shaker-mixer for 30 minutes per bottle of powder. The powders were then manufactured into 3 simple pillar geometries and a hair comb-like structure. All of the specimens were constructed under identical operating conditions via an SLM process in a Concept Laser Mlab unit. For the comb-like structures an "islands" scanning strategy, as detailed in the paper by Keller and Ploshikhin, was used [8]. The purpose of the comb-like structure, shown in Figure 6, was to provide a worst case geometry as it was designed to deform with residual stresses [8]. After the samples were constructed a series of tests were performed to determine various properties, in an attempt to determine which of the three blends produced the highest quality build.

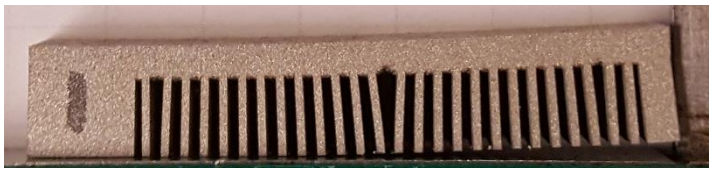

Figure 6: An example of one of the comb-like structures. This comb-like structure is constructed from the 10% 316L powder composition.

Results and Discussion

The first test performed was to determine the density of the pillar geometries. The samples were placed in a degassing chamber for 2 hours and then their densities were measured via the Archimedes method, in accordance with ASTM B311. The results of the density tests, shown in Figure 7, showed a trend of increasing density with increasing 316L content. This trend was expected for two reasons: increasing 316L content is predicted to decrease the amount of delta ferrite present and 316L contains Mo. Delta ferrite is a lower density phase and therefore, the increasing 316L content should have caused a slight increase in overall density. 316L also contains Mo which can increase the density of any delta ferrite present in the matrix thereby increasing the overall density with increasing 316L content. Using JMatPro, simulations were run that predicted an increase in overall density of between 0.06 to 0.08 g/cc from the 10% 316L

blend to the 90% 316L blend; the determined increase was 0.05 g/cc. Based on the Cr/Ni equivalency modeling, it was predicted that the increase in density would be less or non-existent due to the increase in the hot cracking susceptibility that accompanied the increase in Cr/Ni equivalency which would have caused significantly more porosity in the parts.

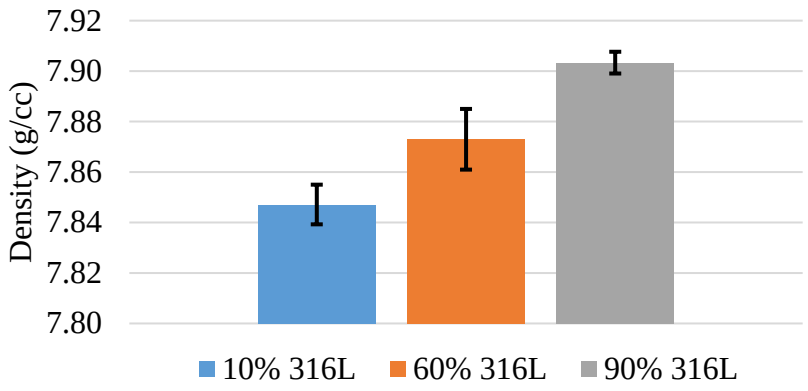

Figure 7: The results of the density measurements of the pillar geometry samples. The measurements were acquired using Archimedes method in accordance with ASTM B311.

To test the degree of distortion each blend underwent, the dimensions of both the pillar geometries and comb-like structures were measured using a fiber laser scanner. The distortion of the pillar samples was determined via a length/width ratio of the measured dimensions. The results of these measurements, shown in Table 3, showed that the 10% 316L and 60% 316L blends had little to no measurable distortion, while the 90% 316L blend had very minor amounts. The distortion of the comb-like samples was determined by measuring the heights of the comb-like structures and then determining the degree of curvature each comb-like structure had. However, the height measurements for the comb-like structures proved to be inconclusive as during the process to remove them from the build plate, the comb-like structures were removed unevenly. This issue also affected the pillar geometries which is the reason no height values were considered.

Table 3: Overall Dimensional Consistency Determined by Laser Scanner

	Length/Width
10% 316L	0.999±0.001
60% 316L	1.001±0.001
90% 316L	0.996±0.001

In addition to density and distortion tests, micrographs were taken of the samples' surface to examine the microstructures present and any micro-cracking that may have occurred. Figure 8, shows a low magnification view of the as-built microstructures of the three comb samples. While Figure 8 appears to show that the 10% 316L blend has less porosity, this is not truly the case. In all blends the porosity was wide spread and common and is believed to be due more to poor build parameters than to material weldability issues.

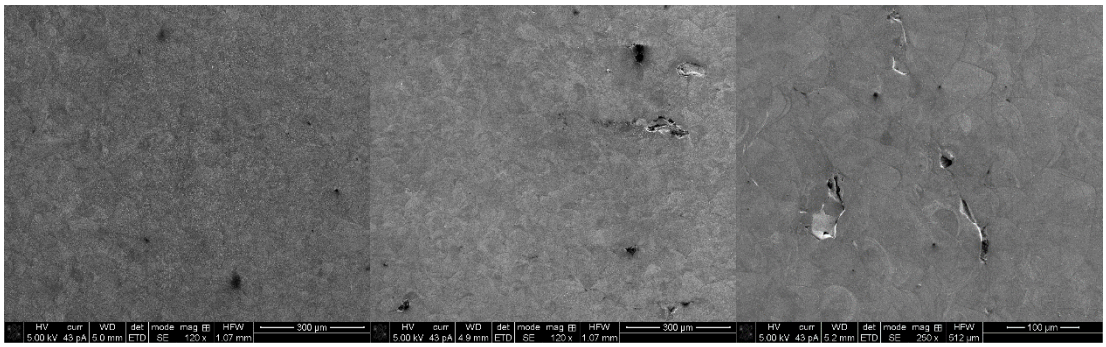

Figure 8: Shows series of SEM micrographs of the comb-like structures for each blend. The 316L content of the blend increases from left to right.

Conclusion

As a preliminary study of using weldability to determine build viability in stainless steel powders for AM, three blended powder compositions were selected. The compositions were selected based on their positions on a modified Schaeffler diagram, created specifically for determining the weldability of materials using Cr/Ni equivalency modeling, and the use of various JMatPro simulations. Once the compositions were selected, the 304L and 316L powders were blended via weight ratio and then homogenized. Each of the blended compositions were then built into 3 simple pillar geometries and one comb-like structure. Each of the samples was then subjected to various tests in order to determine whether any of the blends followed the predicted solidification modes or were subject to the failure modes that the Cr/Ni equivalency modeling predicted. Density measurements were taken on the pillar geometries and showed that as Cr/Ni equivalency increased, the density of the parts increased. Distortion measurements were made using a fiber laser scanner and taking the ratio of length to width for the pillar geometries and then determining the degree of curvature along the spine of the comb-like structures. The results of the distortion measurements on the pillar geometries showed no conclusive trends and the measurements of the comb-like structures were inconclusive. Micrographs of the comb-like structures were examined for micro-cracking and porosity, but all of the powder blend builds appeared to have equivalent build quality.

None of the builds with varying Cr/Ni equivalency exhibited greater evidence of hot tearing or cracking than the others. This suggests that powder bed additive manufacturing may have a wider safe operating range of Cr/Ni equivalency than welding and that the process may be less sensitive to cracking and defect formation than traditional welding processes. The increased density without increasing porosity suggests that AM processes may require the consideration of

additional factors that are not traditionally considered as part of weldability. More work is needed to confirm these results.

Future Work

To further investigate the use of weldability to determine build viability, several additional chemistries need to be tested and additional tests need to be performed. Additional chemistries would help to determine how extreme the Cr/Ni equivalency values can be before the AM parts begin to fail in the manners predicted by Cr/Ni equivalency weldability modeling. More rigorous testing would also allow for a more robust definition of build viability and better determination of which materials are more or less viable for AM processes.

Acknowledgements

This work was funded by Honeywell Federal Manufacturing & Technologies under Contract No. DE-NA0002839 with the U.S. Department of Energy. The United States Government retains and the publisher, by accepting the article for publication, acknowledges that the United States Government retains a nonexclusive, paid up, irrevocable, world-wide license to publish or reproduce the published form of this manuscript, or allow others to do so, for the United States Government purposes.

References

[1] P. S. Korinko and S. H. Malene, “Considerations for the Weldability of Types 304L and 316L Stainless Steel,” vol. 1, no. August, pp. 61–68, 2001.

[2] N. Suutala and T. Takalo, “Ferritic-Austenitic Solidification Mode in Austenitic Stainless Steel Welds,” vol. l, no. May, pp. 717–725, 1980.

[3] B. Y. D. J. Kotecki, “WRC-1992 Constitution Diagram for Stainless Steel Weld Metals : A Modification of the WRC-1988 Diagram,” pp. 171–178, 1992.

[4] F. C. Hull, “Delta Ferrite and Martensite Formation in Stainless Steels,” no. May, 1973.

[5] S. Steel and W. Metal, “The Ferrite Content of Austenitic Stainless Steel Weld Metal,” no. July, 1973.

[6] B. Cla, “A Thermodynamic Study of a Constitutional Diagram for Duplex Stainless Steels,” 2017.

[7] A. S. M. Inc., “AISI Type 316L Stainless Steel, annealed bar,” 2016. [Online]. Available: http://asm.matweb.com/search/SpecificMaterial.asp?bassnum=MQ316Q.

[8] N. Keller and V. Ploshikhin, “NEW METHOD FOR FAST PREDICTIONS OF RESIDUAL STRESS AND DISTORTION OF AM PARTS,” pp. 1229–1237.